Calculation of Rotor Bars Current in Squirrel Cage Induction Motor Under Unbalanced and Harmonic Voltage Conditions Using Multiple-Coupled Circuits

Hamed Shadfar[1], Hamid Reza Izadfar[1*]
1. faculty of Electrical and Computer Engineering Department, Semnan University, Semnan, Iran
hrizadfar@semnan.ac.ir

***Abstract*-- Unbalanced and harmonic voltages are important issues in the power quality field. These factors can have destructive effects on induction motors (IMs and can lead to problems such as high temperature, increased losses, speed and torque fluctuations, and noise in the machine. Therefore, analyzing these factors and their effects on motor performance is very important in the interaction of this machine and the power system. The rotor current is one of the characteristics that is affected by these factors. Calculating the rotor bars current (RBC) using stator data is not easy, but it can be used to predict the behavior of the motor in different conditions. This paper proposes an algorithm based on the repetition method using the stator data based on the multiple-coupled circuits model (MCC) to calculate the RBC in the squirrel cage induction motor (SCIM) under unbalanced and harmonic voltage conditions. For this purpose, a 2-pole SCIM with nominal specifications of 1.1 kW, 220/380 V, and 50 Hz is subjected to experimental testing and simulation. To confirm the practical results, this motor is simulated in the Maxwell software and the results are compared and evaluated with the experimental results.**

***Index Terms*—Harmonic voltage; multiple coupled circuit model; Rotor bars current; Squirrel cage induction motor; Unbalanced voltage.**

I. Introduction

About 70% of electrical energy is used by IMs. In industry, usually about 80% of the load consists of three-phase AC IMs [1]. IMs are used more than ever due to various technical-economic advantages such as versatility, reliability and economy, self-starting, simple structure, easy maintenance and low cost. Although an IM is designed and built to operate in balanced conditions, unfortunately most of them are directly connected to the power distribution system (PDS) and are exposed to unbalanced voltage.

If three-phase IMs have balanced sinusoidal voltages and no harmonics, they can perform well up to their design. However, the supply voltage cannot be balanced or harmonic-free for many technical reasons. Unbalanced voltage can be caused by unbalanced loads, windings or asymmetric transmission impedances, large single-phase loads [2], incomplete transmission of transmission lines, open delta connection of transformer [3], burning fuses in a three-phase capacitor bank, operation of single-phase loads at different times, or faulty transformers in power systems [4]. The unbalanced voltage induces a negative sequence current which in turn creates a reverse rotating field in addition to the forward rotating field produced by the positive sequence. The interaction of these fields causes great problems in the performance of the IM, including pulsating electromagnetic torque and speed disturbances, which lead to an increase in losses, temperature, stresses, and noise in the IM [5-8]. On the other hand, in modern low-voltage networks, many consumers receive non-sinusoidal current from the network. These currents cause a voltage drop due to the network impedance. This causes changes in the shape of the sinusoidal voltage of the network. According to the fast Fourier transform (FFT), these works can be decomposed into the fundamental harmonic of individual harmonics. Harmonic frequencies are integer multiples of the fundamental frequency. The presence of harmonics in the power supply can be caused by: (1) the operation of power electronic devices, (2) the operation of steel mill arc furnaces, and (3) the resonance of shunt capacitors and/or series inductors [9].

When the IM power supply is fed from an inverter or cyclo converter, the motor terminal voltage is non-sinusoidal but has half-wave symmetry. Due to the half-wave symmetry of the inverter output, it will contain only odd harmonics. The harmonics of order (6K+1) have a positive sequence and try to rotate the motor at different speeds in the direction of motor rotation, and the harmonics of order (6K-1) have a negative sequence and try to rotate the motor at different speeds against the direction of motor rotation. The 3rd-order harmonics have zero order. Zero-sequence components are neutral and have no rotation, so any harmonic energy associated with them is dissipated as heat. The torque fluctuations caused by these components can be significant and cause problems with shaft rotational vibration. Therefore, harmonics harm the performance of IMs. These harmonics lead to an increase in the effective value of the current and this leads to an increase in temperature and an increase in losses, a decrease in torque, and noise problems. In addition, high-frequency currents, by induction in the rotor, lead to an increase in losses [10].

According to the above, it is vital to analyze the performance of equipment in power systems, including IMs, in conditions of

voltage imbalance and harmonic voltage. In most cases, condition monitoring schemes are focused on one of three IM components: stator, rotor, or bearings. While little attention has been paid to the problem of unbalanced voltage in the power supply and also the presence of harmonic components in the waveform of the power supply voltage. Due to the widespread use of IM in industrial and domestic applications, the destructive effects on IMs will have an important economic impact. In this paper, an algorithm based on the repetition method using the stator data based on the MCC model is proposed to calculate the RBC in the SCIM under different conditions. It is clear that calculating the RBC is difficult, but it can be used to predict the behavior of the motor in different conditions. In this regard, using the proposed algorithm, the RBC under healthy, unbalanced, and harmonic voltage conditions have been calculated and evaluated.

The rest of the paper is organized as follows. In the second section, the motor modeling based on the MCC model is presented. In the third section, it deals with how to analyze the motor in unbalanced voltage conditions. Also, in the fourth section, the method of analyzing the motor under harmonic voltage conditions is discussed. In the fifth section, the simulation results are examined, and finally, the conclusion is presented in the sixth section.

II. IM MODELING BASED ON THE MCC MODEL

The MCC model was initially introduced in [11] to analyze concentrated winding IMs. This model formulates multiple induction circuits by coupling the stator and rotor of a SCIM. Consider a SCIM having m stator circuits and n rotor bars. The rotor cage is assumed to have n equal loops that are equally spaced, each comprising two rotor bars and the connecting parts of the end rings between them. This configuration is illustrated in Fig. 1. In this circuit, we use an RL model. Since we focus on low frequencies, we can ignore the capacitance between turns and windings. Once we have the values for the parameters, we can calculate the loop currents using standard circuit analysis techniques. Therefore, the equations of the IM can be written as a vector matrix in (1) to (4).

$$V_S = R_S I_S + \frac{d\Lambda_s}{dt} \quad (1)$$

$$V_r = R_r I_r + \frac{d\Lambda_r}{dt} \quad (2)$$

$$\Lambda_s = \mathrm{L}_{ss}\mathrm{I}_s + \mathrm{L}_{sr}\mathrm{I}_r \quad (3)$$

$$\Lambda_r = I_{sr}^T \mathrm{I}_s + \mathrm{L}_{rr}\mathrm{I}_r \quad (4)$$

The L_{sr}^T matrix is the transpose of the L_{sr} matrix. Also:

$$\mathrm{I}_s = [i_{s1}\ i_{s2} \dots\ i_{sm}]^T \quad (5)$$

$$\mathrm{I}_r = [i_{r1}\ i_{r2} \dots\ i_{rn}]^T \quad (6)$$

$$\mathrm{V}_s = [v_{s1}\ v_{s2} \dots\ v_{sm}]^T \quad (7)$$

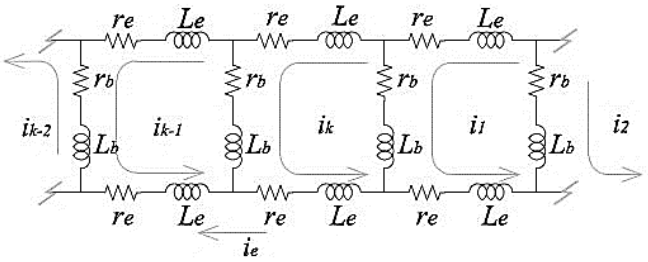

Fig. 1. MCC topology

$$[R_s] = \begin{bmatrix} R_s & 0 & \cdots & 0 & 0 \\ 0 & R_s & \vdots & 0 & 0 \\ \vdots & \vdots & \ddots & \vdots & \vdots \\ 0 & 0 & 0 & R_s & 0 \\ 0 & 0 & \cdots & 0 & R_s \end{bmatrix}_{m\times m} \quad (8)$$

$$[R_r] = \begin{bmatrix} 2(r_b+r_e) & -r_b & 0 & \cdots & -r_b \\ -r_b & 2(r_b+r_e) & -r_b & \cdots & 0 \\ 0 & -r_b & 2(r_b+r_e) & \cdots & \vdots \\ \vdots & \vdots & \vdots & \cdots & \vdots \\ -r_b & 0 & \cdots & \cdots & 2(r_b+r_e) \end{bmatrix}_{n\times n} \quad (9)$$

In the case of the squirrel cage rotor, V_r = [O]. To clarify, it should be noted that the current in the stator and rotor circuits are assumed to be independent. These circuits can then be connected in any way to create the phases of the stator windings and the configuration of the rotor bars and end rings can be considered.

The torque and mechanical equations of the machine are:

$$\frac{d\theta}{dt} = \omega \quad (10)$$

$$\frac{d\omega}{dt} = \frac{1}{J}(\mathrm{T}_e - \mathrm{T}_L) \quad (11)$$

$$\mathrm{T}_e = \frac{1}{2} I_s^T \frac{\partial \mathrm{L}_{ss}}{\partial \theta_r}\mathrm{I}_s + \frac{1}{2} I_s^T \frac{\partial \mathrm{L}_{sr}}{\partial \theta_r}\mathrm{I}_r + \frac{1}{2} I_r^T \frac{\partial \mathrm{L}_{rs}}{\partial \theta_r}\mathrm{I}_s + \frac{1}{2} I_r^T \frac{\partial \mathrm{L}_{rr}}{\partial \theta_r}\mathrm{I}_r \quad (12)$$

where θ is the mechanical angle, ω is the mechanical speed, T_L is the load torque, and J is the rotor inertia.

The calculation of all machine inductances as indicated by the inductance matrices in the above relations is the key to a successful simulation of an IM. These inductances are easily calculated using the winding function theory (WFT). This method does not assume any symmetry in placing each coil in the slots. According to WFT, the mutual inductance between both windings i and j in any electric machine can be calculated using (13) (assuming the permanence of iron is infinite):

$$\mathrm{L}_{ij}(\varphi) = \mu_0 r l \int_0^{2\pi} g^{-1}(\varphi.\theta) N_i(\varphi.\theta) N_j(\varphi.\theta) d\theta \quad (13)$$

Where φ is the angular position of the rotor relative to the stator reference, θ is a specific angular position along the inner surface of the stator, $g^{-1}(\varphi.\theta)$ is called the inverse of the distance function, which becomes l/g assuming the air gap is uniform. l is the stack length and r is the average radius of the air gap. $N_i(\varphi.\theta)$ is the winding function. Therefore, it is possible to calculate the RBC [12].

III. PROCESS OF CALCULATING THE RBC

The process of calculating the RBC in the proposed method using the stator data and modeling the motor based on the MCC

is shown in Fig. 2. This algorithm is programmed in Matlab software. Its input is the nominal specifications of the studied motor and stator data, and its output is the various characteristics of the motor, including the RBC.

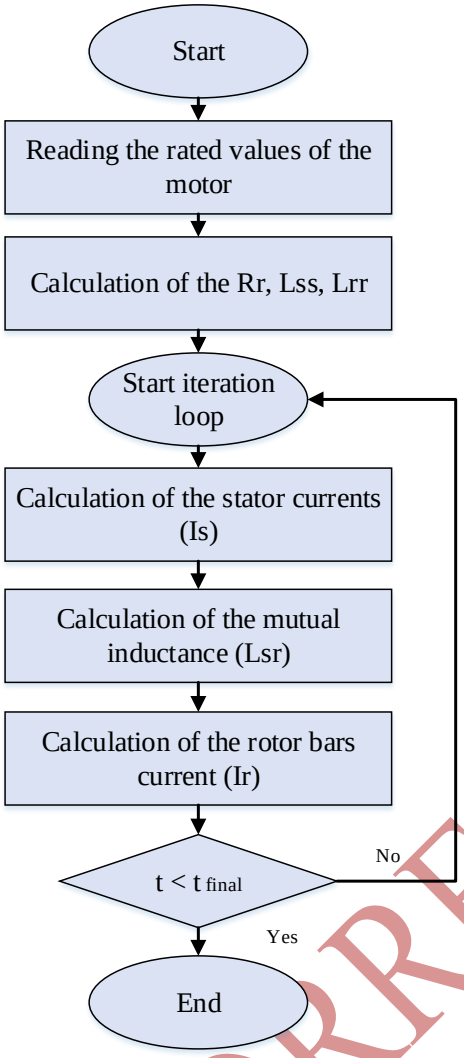

Fig. 2. Flowchart of the calculation process of RBC

IV. MOTOR ANALYSIS UNDER UNBALANCED VOLTAGE CONDITION

Unbalanced Voltage is a phenomenon that is related to changes in three-phase PDS patterns [13]. This pattern is provided by a balanced system, consisting of voltages of equal magnitude and 120 electrical degrees lagged each other. An appropriate standard must be used to quantify the degree of voltage unbalance. Various definitions of voltage unbalance have been proposed.

A. NEMA standard

The voltage unbalance according to the NEMA standard, which is also known as the line voltage unbalance rate (LVUR), is expressed as (14) [14].

$$\%LVUR = \frac{max\ voltage\ deviation\ from\ average\ line\ voltage}{average\ line\ voltage} \times 100 \quad (14)$$

B. IEEE standard

The IEEE definition of voltage unbalance, which is also known as phase voltage unbalance rate (PVUR), is expressed as (15) [15].

$$\%PVUR = \frac{max\ voltage\ deviation\ from\ average\ phase\ voltage}{average\ phase\ voltage} \times 100 \quad (15)$$

C. IEC standard

Another definition of voltage unbalance is given as the ratio of the negative sequence voltage component to the positive sequence voltage component. The percentage of voltage unbalance coefficient (% VUF) is presented according to (16) [16].

$$\%VUF = \frac{negative\ sequence\ voltage\ component}{positive\ sequence\ voltage\ component} \times 100 \quad (16)$$

V. MOTOR ANALYSIS UNDER HARMONIC VOLTAGE CONDITIONS

Harmonic voltage distortions are phenomena that are associated with changes in the waveform of voltages and currents to the fundamental frequency of the sinusoidal wave [17]. The distortion of the voltage source is alternating and can be decomposed into an infinite sequence of sinusoidal waves by applying the FFT. Considering k = 0, 1, 2, 3, ..., we have harmonics with positive, negative, and zero sequences.

The applied voltage can be written as (17):

$$V(t) = V_1 \sin(2\pi ft) + \sum_{k=3.5.7} V_k \sin(2\pi ft + \theta_k) \quad (17)$$

Based on (17), it is expected that there are harmonics with the same frequency but different amplitude in the stator current.

VI. SIMULATION RESULTS

A SCIM, whose parameters are given in Table I, is investigated in this paper. The stator winding connection is Y. This motor is evaluated and experimental tested under balanced voltage, unbalanced voltages, and harmonic voltage conditions. Figure 3 shows a picture of the laboratory set. Also, to confirm the experimental results, the simulation results of this motor have been used in the Ansys Maxwell software based on the FEM.

Table I
Characteristics of the studied SCIM

Parameter	**Specifications**
Power (kW)	1.1
Voltage (V)	380
Frequency (Hz)	50
Speed (RPM)	2850
Nominal Current (A)	2.46
Pole number	2
Number of stator slot	18
Number of rotor bars	16

Air gap length (mm)	1
The inner diameter of the stator core (mm)	67
The outer diameter of the stator core (mm)	121
Number of conductors per stator slot	85
Stator core length (mm)	76
Skew angle of rotor bars (degrees)	5

Fig. 3. Laboratory set to calculate the rotor bars' current

A. Unbalanced voltage

Doing so is necessary to establish a reference for comparison purposes of motor performance under normal and unbalanced voltage conditions. Considering that according to the standard in the PDS, the voltage drop in each phase is acceptable up to a maximum of ±5%, for this purpose according to the IEEE standard, unbalanced voltages (only the magnitude changes and phase angle is fixed) are applied to the motor according to Table II.

By applying the conditions mentioned in Table II to the studied motor under the torque of 3.5 Nm, the current waveform of the stator phases is shown in Fig. 4. Also, the heating of the stator and especially the rotor, reduces the efficiency and possibly leads to faster thermal aging.

Table II
Different studied modes of voltage unbalance

Phase	Balanced voltage	Unbalanced voltage (state1)	Unbalanced voltage (state2)
A	322	322	322
B	322	306	338
C	322	314	306
%PVUR	0	2.5	5

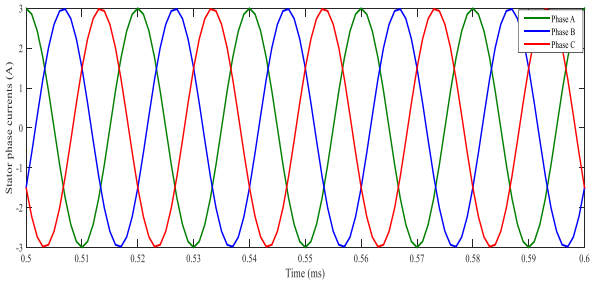

(a)

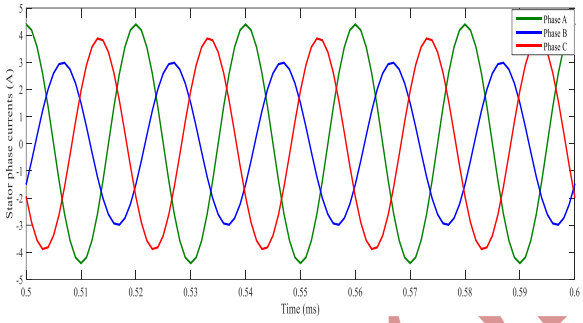

(b)

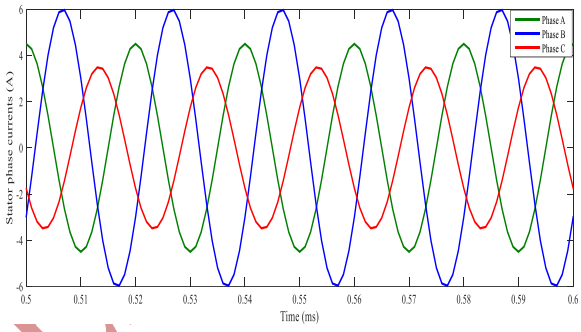

(c)

Fig. 4. Current waveform of stator phases (a) balanced voltage, (b) unbalanced voltage (state1) and (c) unbalanced voltage (state2)

It is clear that the voltage unbalance will lead to the current unbalance and also increase the current amplitude in each phase. This causes the motor to overcurrent and as a result, overheat. Also, it will reduce the life of the motor.

The RBC under the above conditions at time t=500 ms is shown in Fig. 5. Also, as an example of the current of one of the rotor bars, it is shown in Fig. 6. It can be seen that in the condition of voltage imbalance, the current range of the rotor bars has increased. In addition, the voltage unbalance leads to fluctuations in the current waveform of the rotor bars. These fluctuations have increased with the increase in unbalance percentage.

Figure 7 shows the flux density curve in the air gap under the mentioned conditions. Also, in Fig. 8, the FFT of the flux density curves in the air gap in different conditions is presented. The THD of the flux density in the condition of balanced voltage and voltage imbalance of the first and second state is equal to 20, 22, and 26%, respectively. This shows that voltage unbalance, in addition to reducing the level of flux density, leads to an increase in its distortion.

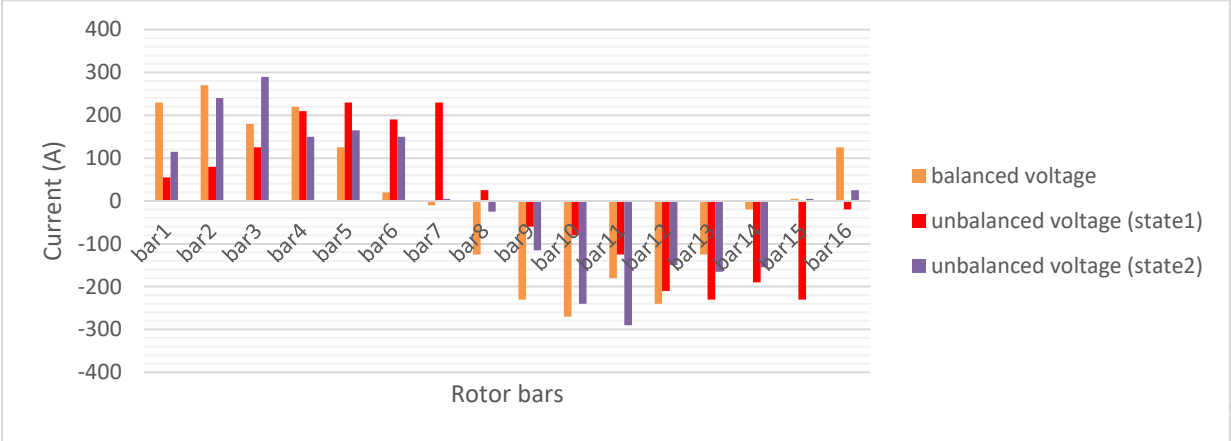

Fig. 5. Current of rotor bars in balanced and unbalanced voltage conditions

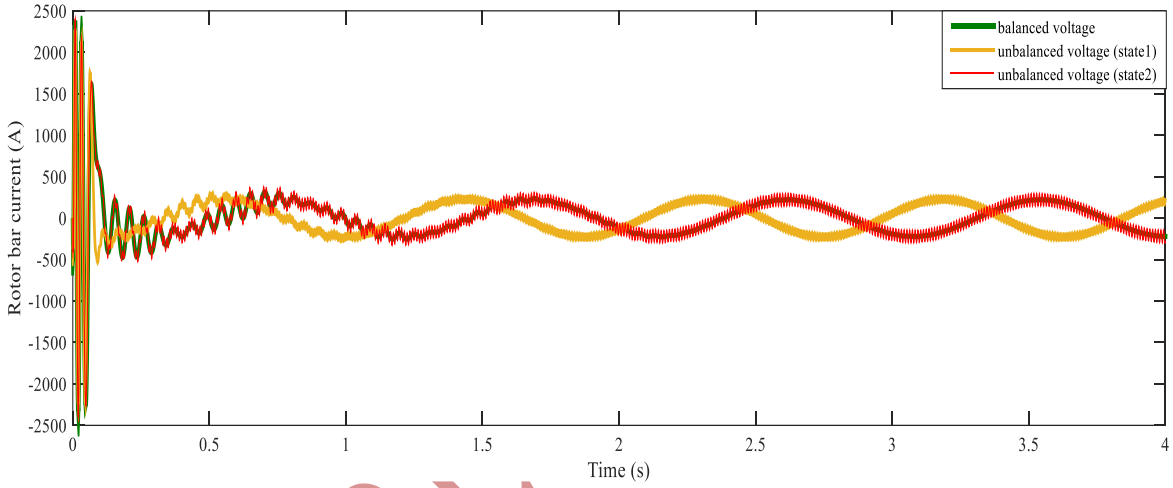

Fig. 6. Current waveform of a rotor bar in different conditions

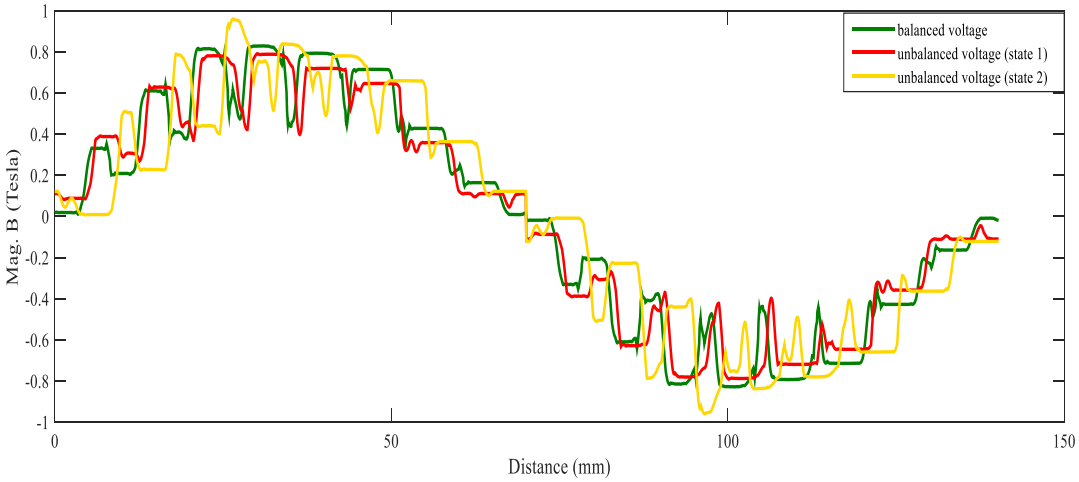

Fig.7. Flux density distribution curve in balanced and unbalanced voltage conditions

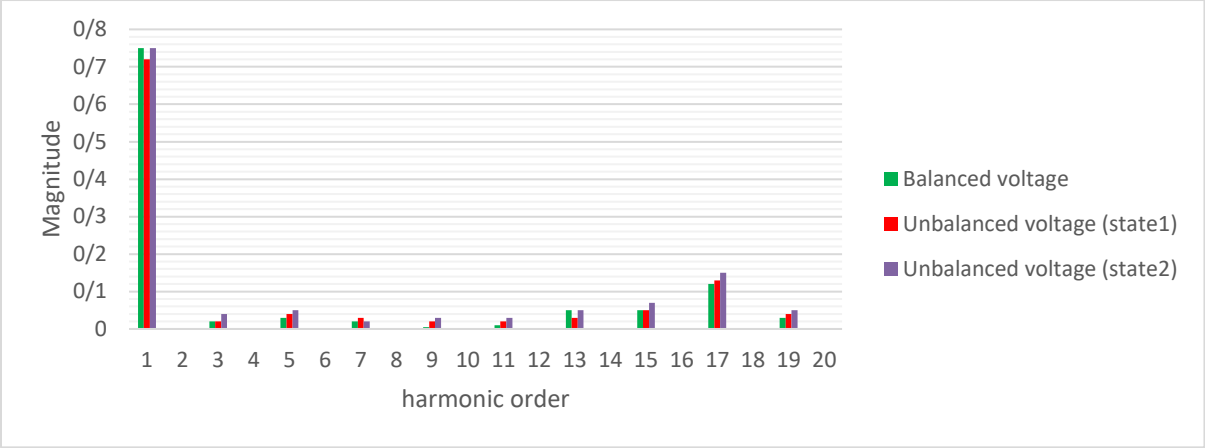

Fig. 8. Harmonic components of flux density in balanced and unbalanced voltage conditions

B. Harmonic voltage

Investigating the effect of harmonics in the output voltage of the drive on the performance of the SCIM is the aim of this section. For this purpose, according to Fig. 9, we ran the studied motor under no-load conditions by the drive and measured its input voltage. The waveform of phase A is shown in Fig. 10. The harmonic voltage of the stator will lead to the generation of harmonic current. Therefore, the input current of the motor will be as shown in Fig. 11.

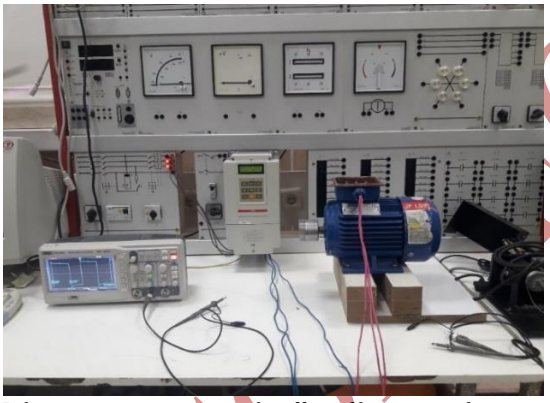

Fig.9. Laboratory set to investigate the effect of harmonic voltage

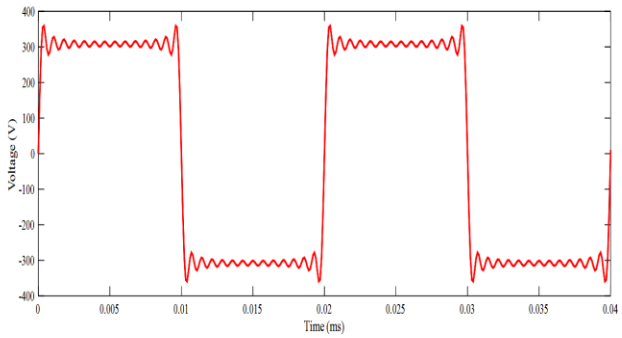

Fig.10. Drive output voltage waveform (phase A)

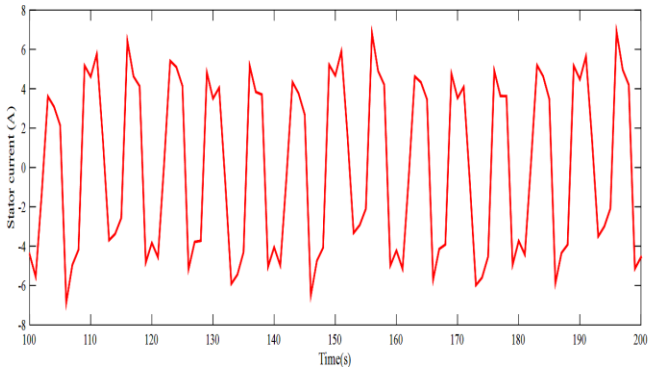

Fig.11. Stator phase current waveform (phase A)

In this condition, the current of the rotor bars at time t=200 ms is calculated and presented in Fig. 12. As an example, the current of one of the rotor rods is shown in Fig. 13. As can be seen, the harmonic voltage of the stator has led to an increase in the current amplitude of the rotor bars. In addition, according to Fig. 13, the THD in the current waveform of the rotor bars has increased greatly.

Figure 14 shows the flux density curve in the air gap under the mentioned conditions. Also, in Fig. 15, the FFT of the flux density curves in the air gap in different conditions is presented. The THD of the flux density in the starting conditions without the drive and with the use of the drive is equal to 17 and 25%, respectively. Therefore, it can be concluded that the harmonic stator voltage will lead to the harmonic stator current. This will lead to the harmonic air gap field and ultimately the harmonic rotor current.

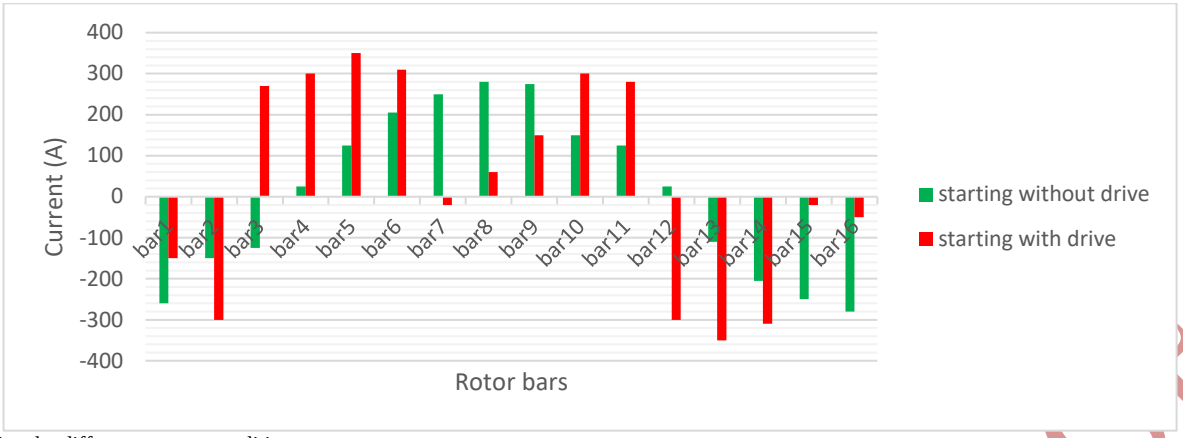

Fig.12. RBC under different start-up conditions

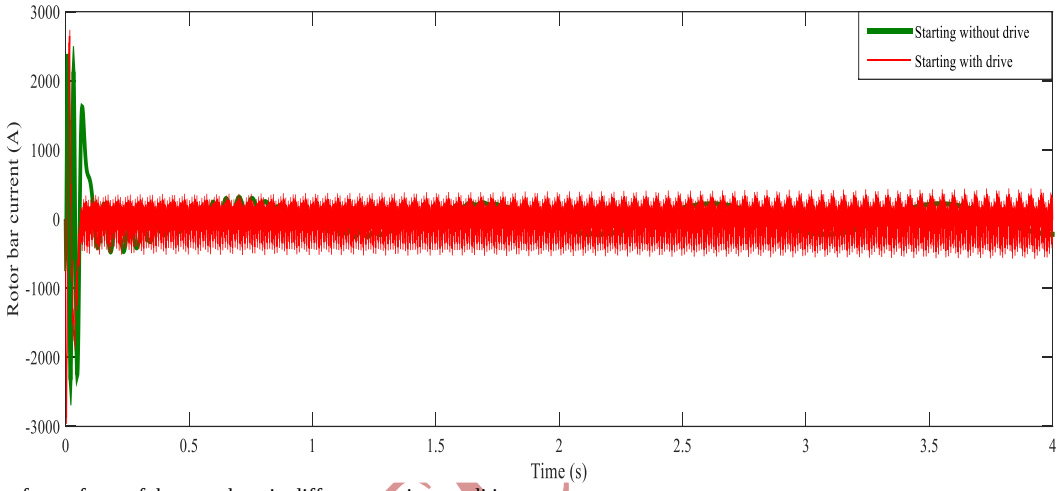

Fig.13. Current waveform of one of the rotor bars in different starting conditions

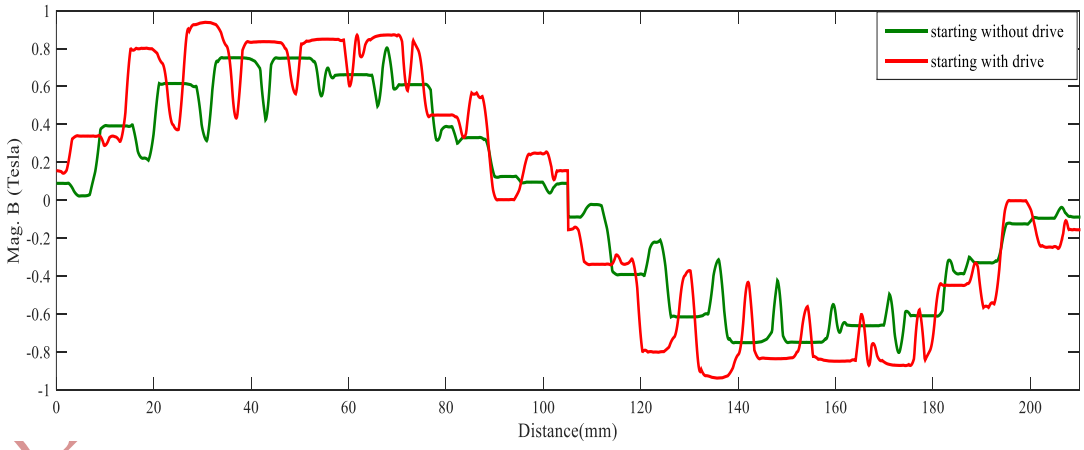

Fig.14. Flux density distribution curve in different starting conditions

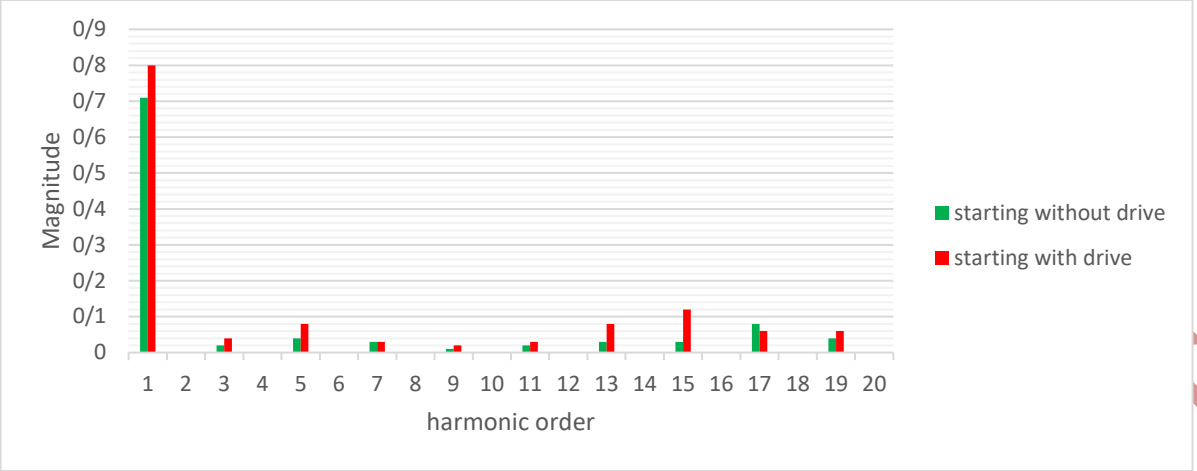

Fig.15. harmonic components of flux density in different starting conditions

VII. CONCLUSION

In this paper, a comprehensive and general method for calculating the RBC using stator data is presented to predict the steady-state performance of three-phase SCIM under unbalanced voltage and harmonic voltage conditions. This prediction can make the IM control system especially suitable for damage prevention in high-power machines. It is well known that voltage unbalances and harmonics cause additional loads to installations and additional costs to consumers. Therefore, detecting these abnormal conditions in the machine is very important in the interaction between the electric machine and the power grid. The analysis of the test results shows that the negative effects of the unbalanced sinusoidal voltage, which is always present in the power supply, are greater than the balanced non-sinusoidal voltage (inverter supply) on the performance of the IM.

The comparison of practical tests and simulation results shows that the proposed method can be used as an effective method in detecting abnormal conditions of the IM.

REFERENCES

[1] O. Souto, J. Oliveira, and L. Neto, “Induction motors thermal behavior and life expectancy under nonideal supply conditions,” in IX Int. Conf. Harmonics and Quality of Power, Orlando, FL, 2000.
[2] D. Mirabbasi, G. Seifossadat, and M. Heidari, "Effect of unbalanced voltage on the operation of induction motors and its detection," in ELECO 2009. International Conference on Electrical and Electronics Engineering, Bursa, 5-8 Nov. 2009.
[3] C.-Y. Lee, W.-J. Lee, Y.-N. Wang and J.-C. Gu, "Effects of voltage harmonics on the electrical and mechanical performance of a three-phase induction motor," in IEEE Industrial and Commercial Power Systems Technical Conference, Edmonton, Alta., 3-8 May 1998.
[4] A. G. Siraki and P. Pillay, "An In Situ Efficiency Estimation Technique for Induction Machines Working With Unbalanced Supplies," IEEE Transactions on Energy Conversion, vol. 27, no. 1, pp. 85-95, March 2012.
[5] Mirabbasi, Davar, Ghodratollah Seifossadat, and Mehrdad Heidari. "Effect of unbalanced voltage on the operation of induction motors and its detection." In 2009 International Conference on Electrical and Electronics Engineering-ELECO 2009, pp. I-189. IEEE, 2009.
[6] A. B. Neves, A. L. F. Filho, and M. V. B. Mendonca, “Effects of voltage unbalance on torque and efficiency of a three-phase Induction motor”, 16th IEEE conf. on Harmonics and Quality of Power, May 2014, pp. 679 – 683.
[7] E. C. Quispe and I. D. Lopez, “Effects of unbalanced voltages on the energy performance of three phase induction motors”, IEEE conf. on Power Electronics and Power Quality Applications, July 2015, pp. 1-6.
[8] "IEEE Guide for AC Motor Protection," IEEE Std C37.96-2000, pp. 1-112, Sept. 8 2000.
[9] J. M. Corres, J. Bravo, F. J. Arregui and I. Matias, "Unbalance and harmonics detection in induction motors using an optical fiber sensor," IEEE Sensors Journal, vol. 6, no. 3, pp. 605-612, June 2006.
[10] ANSI/NEMA, "American National Standard Motors and Generators, ANSI/NEMA MG 1-2011, Revision of ANSI/NEMA MG 1-2010,"American National Standards Institute, Inc., 2011.
[11] H. Toliyat, T. Lipo, J. White, Analysis of a concentrated winding induction machine for adjustable speed drive applications: I. Motor analysis, IEEE Trans.Energy Convers. 6 (4) (1991) 679–683.
[12] H. Toliyat, T. Lipo, Transient analysis of cage induction machines under stator and rotor bar and end ring faults, IEEE Trans. Energy Convers. 10 (2) (1995) 241–247.
[13] Donolo, Pablo, Guillermo Bossio, and Cristian De Angelo. "Analysis of voltage unbalance effects on induction motors with open and closed slots." Energy Conversion and Management 52, no. 5 (2011): 2024-2030.
[14] Motors and Generators, ANSI/NEMA Standard MG1-1993.
[15] IEEE Standard “Test Procedure for Polyphase Induction Motors and Generators”, IEEE Standard 112, 1991.
[16] W.A Elhaija, A. Muetze “A voltage unbalance factor coding technique for three phase induction motors” Int Trans Electr Energ Syst. 2018.
[17] Neves, A. B. F., de Mendonça, M. V. B., de Leles Ferreira Filho, A., & Rosa, G. Z. (2016, October). Effects of voltage unbalance and harmonic distortion on the torque and efficiency of a Three-Phase Induction Motor. In 2016 17th International Conference on Harmonics and Quality of Power (ICHQP) (pp. 943-948). IEEE.